International Journal of Mass Spectrometry 278 (2008) 69–74

Contents lists available at ScienceDirect

International Journal of Mass Spectrometry

journal homepage: www.elsevier.com/locate/ijms

Visible wavelength MALDI using Coumarin laser dyes

X.K. Hu [a], D. Lacey [a], J. Li [a], C. Yang [a], A.V. Loboda [b], R.H. Lipson [a,*]

[a] Department of Chemistry, University of Western Ontario, London, ON N6A 5B7, Canada
[b] MDS Analytical Technologies, 71 Four Valley Drive, Concord, ON L4K 2V8, Canada

ARTICLE INFO

Article history:
Received 23 June 2008
Received in revised form 14 August 2008
Accepted 18 August 2008
Available online 26 August 2008

Keywords:
Visible wavelength MALDI
Coumarin dye
C510
C519
Mechanism

ABSTRACT

Experiments are described that assess the viability of visible-matrix assisted laser desorption ionization (MALDI), and provide insight into its mechanism. Organic laser dyes Coumarin 510 and 519 were used as matrixes for the first time to record visible-MALDI mass spectra in both positive and negative ion modes. Coherent radiation between 355 nm and 520 nm was generated using an optical parametric oscillator (OPO), and the resultant MALDI ions were mass recorded in a triple quadrupole mass spectrometer. The Coumarin matrixes exhibit less fragmention when excited with visible light compared to ultraviolet (UV) radiation resulting in less background noise across the mass range of the spectrometer. A detailed examination of the effects of laser fluence and wavelength on C510 was carried out. The slopes of the log–log plots of signal versus fluence at low fluences are ~9 and decrease significantly at higher fluence levels. This behavior is similar to what is observed using both infrared and ultraviolet sources, and suggest that the ionization process is enabled by the presence of ionizing particles activated by thermal energy deposited into the matrix.

1. Introduction

The vast majority of matrix assisted laser desorption ionization (MALDI) mass spectrometry has been carried out using either ultraviolet (UV) or infrared (IR) lasers. In some cases, IR-MALDI has been shown to be superior to UV–MALDI, resulting in less fragmentation, particularly for unstable compounds [1,2] although usually much higher pulse energies are required. Although the mechanism(s) leading to MALDI ions are still controversial, the mass spectra obtained using both UV and IR wavelengths are often very similar. This observation has led some to infer that a single MALDI mechanism operates in both wavelength regions [3]. Others however have pointed out that the similarities of the resultant spectra are more indicative of the final ion states, and not the initial states of the ion precursors [4] because the UV and IR wavelengths excite different types of transitions; namely, electronic and vibrational, respectively. This suggests that secondary reactions are so dominant that the primary ionization events are simply not reflected in the final distribution of ions observed [5]. Thus, even if different primary ions are generated at different incident wavelengths, the secondary reactions in the MALDI plume will convert the initial primary ions to the most thermodynamically favorable secondary products, resulting in similar final mass spectra.

Comparatively few MALDI studies have been reported using visible wavelengths even though many macromolecules of interest are transparent in this spectral region, and therefore will not directly absorb the radiation and fragment. Early studies were published on the potential of Rhodamine dyes [6,7] and Neutral Red [8] as possible matrixes for visible MALDI. Similarly, the use of binary liquid mixtures of Rhodamine 6G dissolved in either 3-nitrobenzyl alcohol (NBA) or glycerol, using 532 nm laser radiation to desorb peptides and proteins, was also explored [9]. More recently, Kim et al. described surface-assisted desorption/ionization mass spectrometry, (SALDI-MS), where biomolecules co-deposited on a graphite surface with glycerol acting as a protonation source were desorbed using 532 nm light [10]. Neutral Red adsorbed onto the surface of gold nanoparticles has also been used as a matrix for UV SALDI to characterize aminothiols [11]. Some Coumarin laser dyes (Coumarin 2, 47, 120, and 152) have been tested for conventional UV–MALDI using a N_2 laser operating at 337 nm [12,13]. Similar studies however have not been reported using Coumarin dyes as matrixes for visible-MALDI.

It is surprising that more work has not been done on visible-MALDI because less fragmentation is expected using longer wavelengths. This may be because UV–MALDI has been so successful using a limited number of matrixes optimized primarily for N_2 laser irradiation. However, matrix fragmentation makes UV experiments problematic for small drug analysis. The motivation for this paper is to begin a rational exploration of the properties of visible-MALDI to establish if there are any genuine advantages in working in the visible, if there any class of visible-absorbing

* Corresponding author.
E-mail address: rlipson@uwo.ca (R.H. Lipson).

1387-3806/$ – see front matter © 2008 Elsevier B.V. All rights reserved.
doi:10.1016/j.ijms.2008.08.009

matrix compounds that are as generic as those used in the UV such as 2,5-dihydroxy benzoic acid (DHB), α-cyano-4-hydroxycinnamic acid (CHCA), and sinapinic acid (SA), and if possible, obtain some insight into the MALDI mechanism as the visible lies between the IR and UV.

In this paper visible-MALDI spectra of the different analytes are reported, using Coumarin 510 (C510; $C_{20}H_{18}N_2O_2$, 2,3,6,7-tetrahydro-10-(3-pyridinyl)-1H,5H,11H-[1]benzopyrano [6,7,8-ij]quinolizin-11-one, molecular mass, MM = 318 g mol^{-1}) and Coumarin 519 (C519; $C_{16}H_{15}NO_4$, 2,3,6,7-tetrahydro-11-oxo-1H,5H,11H-[1]benzopyrano[6,7,8-ij]quinolizine-10-carboxylic acid, MM = 285.29 g mol^{-1}) laser dyes as matrixes. The absorption maxima of these dyes lie in the blue region of the visible spectrum. Incident wavelengths between 355 nm and 520 nm were used to correlate the intensity of the MALDI signals with the absorption spectra of the dyes. The effect of laser fluence was also investigated to glean an insight into the MALDI mechanism as the visible wavelengths used in this work bridge the spectral region between the UV and IR.

2. Experimental/materials and methods

The experimental arrangement used to record MALDI mass spectra has been reported elsewhere [14]. Briefly, in these experiments a MALDI mass spectrometer was built by replacing the front end of an Applied Biosystems/MDS Sciex API-365 LC/MS/MS triple quadrupole (QqQ) mass spectrometer originally configured for electrospray ionization (ESI) with a home-made MALDI ion source. All spectra were obtained by scanning the first quadrupole (Q_1) across the mass range of 50 to ∼2200 Da and averaged over multiple laser shots. MALDI ions were detected (in either positive or negative mode) with a channeltron electron multiplier (Burle Industries). During the experiments, the pressure of N_2 gas introduced into the ionization region was set to 10 mTorr to cool the ions and enable collisional focusing in Q_0.

Laser pulses at different visible wavelengths were generated by an optical parametric oscillator (OPO) (Quanta Ray, model MOPO-HF) pumped by an injection-seeded pulsed Nd:YAG laser, Quanta Ray Model, PRO-250. Laser energies between 5 μJ and 120 μJ per pulse were measured with a NOVA Laser Power/Energy Monitor (OPHIR). The beam was introduced into a 200 μm diameter optical fiber using a 5 cm focal length lens, and focused onto the face of the sample probe placed at an angle of ∼30° to the direction of beam propagation (spot size ∼0.2 mm in diameter). This created a plume of material from the surface of the probe that expanded outward along the axis of the mass spectrometer.

The wavelengths used in the MALDI experiment were chosen to match the UV–visible absorption spectra of the dye matrixes. The MALDI sample probe was rotated continuously at a rate of ∼5 rotations per minute (rpm). Because the laser beam position was fixed, a typical scan left an obvious ablation ring on the sample probe. The ring dimensions were used to calculate the average amount of analyte consumed during a scan. Typically, over 1000 laser shots on a single ring completely consumed the sample and ensured that the MALDI ion signals recorded were comparable at different laser fluences.

The analyte used in these visible wavelength MALDI experiments were the peptides Dalargin (MM = 725.8 g mol^{-1}) and Bradykinin (MM = 1060.2 g mol^{-1}), as well as Adrenocorticotropic Hormone (ACTH) 1–17 clip (MM = 2093.0 g mol^{-1}). Each analyte was > 97% pure, and used as is in a 30:70 water:acetonitrile solution. The Coumarin dyes used as matrixes, C510 and C519 (Exciton), were also used without further purification. 50 mM solutions of C510 were prepared using a solvent that was an equivolume mixture of acetonitrile/methanol with 0.1% by volume trifluoroacetic acid (TFA) added. Similarly, saturated C519 solutions (<50 mM) with the same solvent were used. For experiments mixtures of 60 μL of Coumarin dye solution and 10 μL of 1 mM Dalargin, 2 mM Bradykinin or 0.5 mM ACTH solution were spotted on a 10 mm-diameter sample probe. The sample mixtures were air dried before insertion into the MALDI instrument.

The UV–visible spectra of ∼1 mmol Coumarin dye solution were recorded using a Varian Cary 50 spectrometer. The diffuse reflectance spectra of the solid solution were obtained with a Varian Cary 100 spectrometer equipped with a Varian diffuse reflectance attachment.

3. Results and discussion

3.1. Observed spectra in positive ion mode

The chemical structures of C510 and C519 are shown in Fig. 1. While the C510 molecule has no obvious proton-donating functional groups, the C519 molecule contains a carboxylic acid group that can serve in this capacity. Yet both dye molecules function well as MALDI matrixes. It can therefore be concluded that possessing a functional group capable of proton donation is not a strict criterion for matrix selection. There are several possible reasons for this; the matrix molecule becomes a better proton donor in its excited states, or protonation occurs via a matrix molecular fragment or matrix cluster species.

As shown in Fig. 2 C510 works well at λ = 480 nm as a matrix for the different analytes studied in this work. The upper mass range that could be explored was limited by the mass spectrometer. The Coumarin matrixes were characterized by selecting Dalargin to record MALDI spectra under different experimental conditions. Typical mass spectra using 480 nm light are shown in Fig. 3(a) and (b), respectively. Both mass spectra were taken using laser energy of 60 μJ per pulse. In both spectra, a protonated

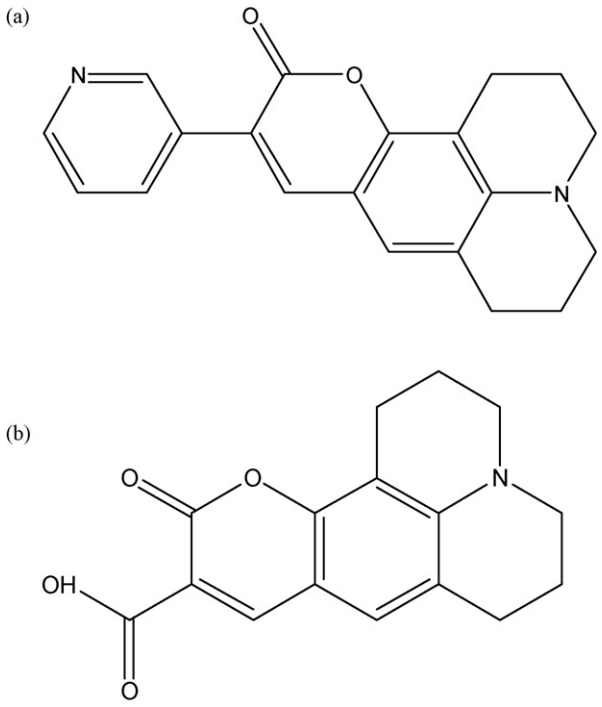

Fig. 1. Chemical structure of (a) Coumarin 510 (C510) with molar mass = 318.00 g mol^{-1} and (b) Coumarin 519 (C519) with molar mass = 285.29 g mol^{-1}.

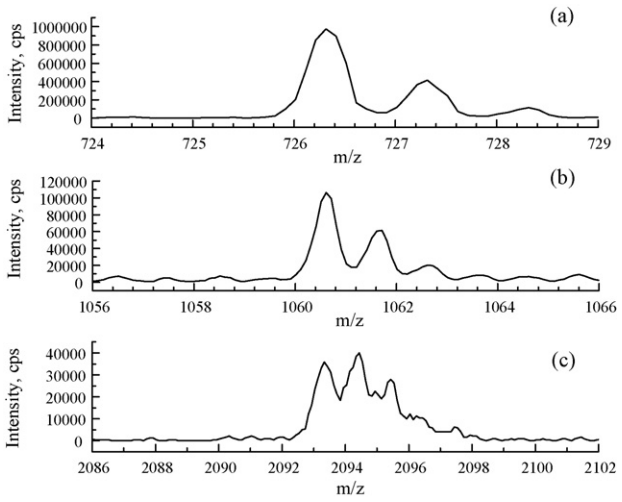

Fig. 2. Visible MALDI spectrum of (a) Dalargin, (b) Bradykinin, and (c) ACTH (1–17 clip) using C510 as matrix.

Dalargin peak is observed. Neither doubly charged Dalargin ion signals [Dalargin+2H]$^{2+}$, Dalargin fragments, nor the Dalargin radical cation were visible.

A signal attributed to protonated C510 ([C510+H]$^+$; $m/z = 319$) is the dominant feature in Fig. 3(a) indicating that the C510 molecule for the most part remains intact under 480 nm irradiation. In the case of C519, the dominant feature that occurs at $m/z = 268$ is assigned to protonated but dehydrated C519 (C519+H$^+$−H$_2$O). Weaker signals of C510 and C519 dimers are also seen. The C510 dimer peaks are more intense than those of C519. Higher order clusters are not evident. While both C510 and C519 can fragment producing low molecular weight ions this mass region is relatively cleaner than that obtained by conventional UV–MALDI. Overall, the MALDI spectra obtained using C510 were found to be superior to those recorded using C519. The S/N ratios in Fig. 3 for C510/Dalargin and C519/Dalargin at 1 Da resolution (mass spectrometer limited) were 165:1 versus 13:1 at the protonated Dalargin mass signal.

The matrix to analyte ratio in MALDI can dramatically affect the relative analyte and matrix signal intensities. For example, matrix signals can be entirely suppressed if the analyte concentration is sufficiently high [15,16]. In the present experiments, the mass spectra with the best signal-to-noise ratio were recorded with a C510: Dalargin mole ratio of 300:1. A similar ratio was obtained for C519.

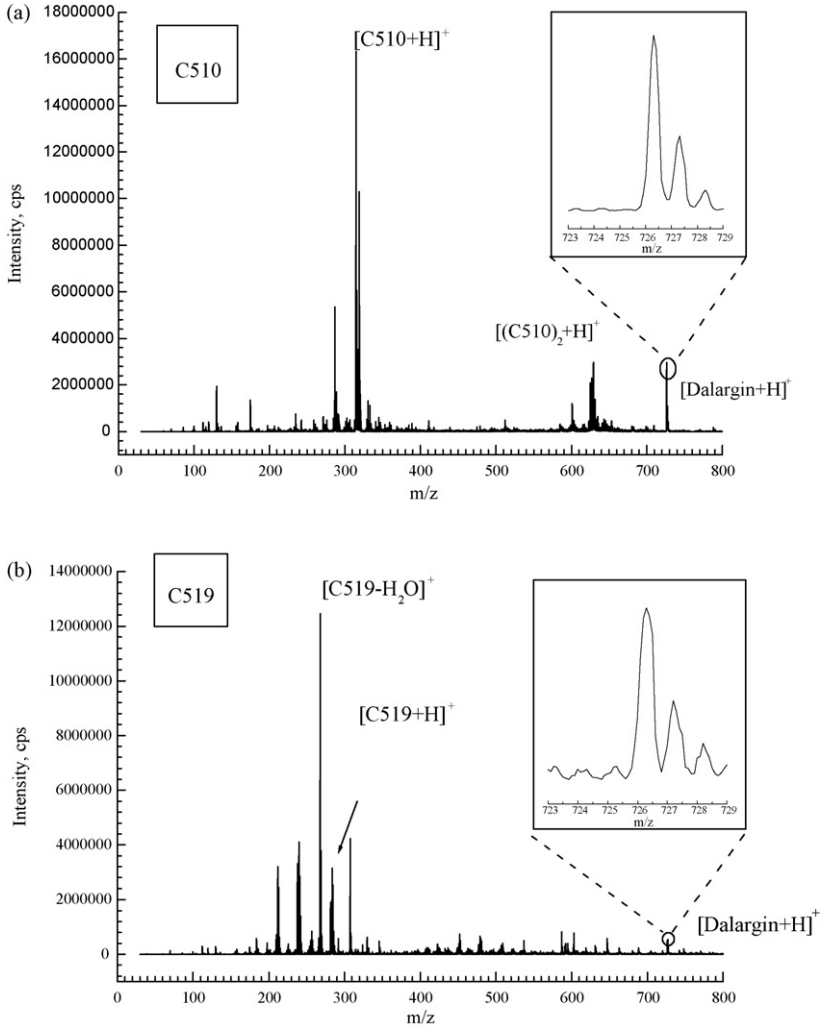

Fig. 3. Visible MALDI spectrum of Dalargin using (a) C510 and (b) C519 as matrixes. Intensity units are in counts per second, cps. The spectrum was recorded using 480 nm photons and an incident laser energy of 60 μJ per pulse.

A detection limit of 1.65 ± 1 pmol was obtained by extrapolating a plot of signal-to-noise ratio versus absolute analyte concentration in the laser spot. The signal used in determining the signal-to-noise ratio was the Dalargin peak maximum at $m/z = 726.4$, while the noise was determined by measuring the average value of the pure noise level between $m/z = 724$ and 726. This average reflected both instrumental noise, and the chemical noise due to the matrix. A value of the signal-to-noise ratio = 5 was considered as a minimum value that would allow the peak signal to be clearly differentiated from the noise, thereby giving an indication of the lowest concentration that can be measured reliably above the background. A similar detection limit was determined by using C519 as a matrix. Although these detection limits are orders of magnitude higher than the best reported in the literature, they are comparable to those obtained with the instrumentation used in this lab by UV–MALDI. However, it should be appreciated that the absolute signals and noise are approximately one order of magnitude higher using UV irradiation [17]. We anticipate that a better comparison could be obtained using a TOF instrument.

3.2. Visible-MALDI in negative ion mode

The structure of C510 contains four sites that can act as proton acceptors. A typical negative ion spectrum for Dalargin, taken at 480 nm with 60 μJ pulse energy, is shown in Fig. 4(a). The samples were prepared in the same manner as those employed in the positive ion mode, and the spectra were obtained under similar experiment conditions.

Deprotonated Dalargin ion signals $[Dalargin\text{-}H]^-$, are readily seen and the matrix interference is considerably less than that observed in positive ion mode. Although deprotonated C510 ($[C510\text{-}H]^-$) is also visible at $m/z = 317$, the strongest feature in the spectrum is a mass peak at $m/z = 112.1$. The neutral mass of this fragment ($m/z = 113.1$) corresponds to $C_6H_9O_2$ which could be 2-methyl-2-pentenoic acid. However this remains to be confirmed. Due to its relative high intensity, it can be speculated that this fragment is the species that protonates C510 and Dalargin, and may be related to one of the rings of the molecule. That would be consistent with the species being an acid.

Since C519 can act as a proton acceptor as well as a proton donor, MALDI mass spectra of deprotonated Dalargin in C519 were also recorded in negative ion mode. A typical spectrum, taken at an incident wavelength of 480 nm with a pulse energy of 60 μJ, is shown in Fig. 4(b). There is again, less interference from the matrix when the spectrum is recorded in negative ion mode. The deprotonated Dalargin mass peak at $m/z = 724.3$ is about 10 times stronger than that recorded in positive ion mode. The deprotonated C519 molecule is also readily seen at $m/z = 284$ although the strongest feature in the spectrum is now assigned to $m/z = 240$ which corresponds to C519 with its carboxylic acid group removed $[C519\text{–}COOH]^-$. The same mass peak at $m/z = 112.1$ observed in C510 negative ion MALDI spectrum was also observed here indicating this species is a common fragment of both dyes.

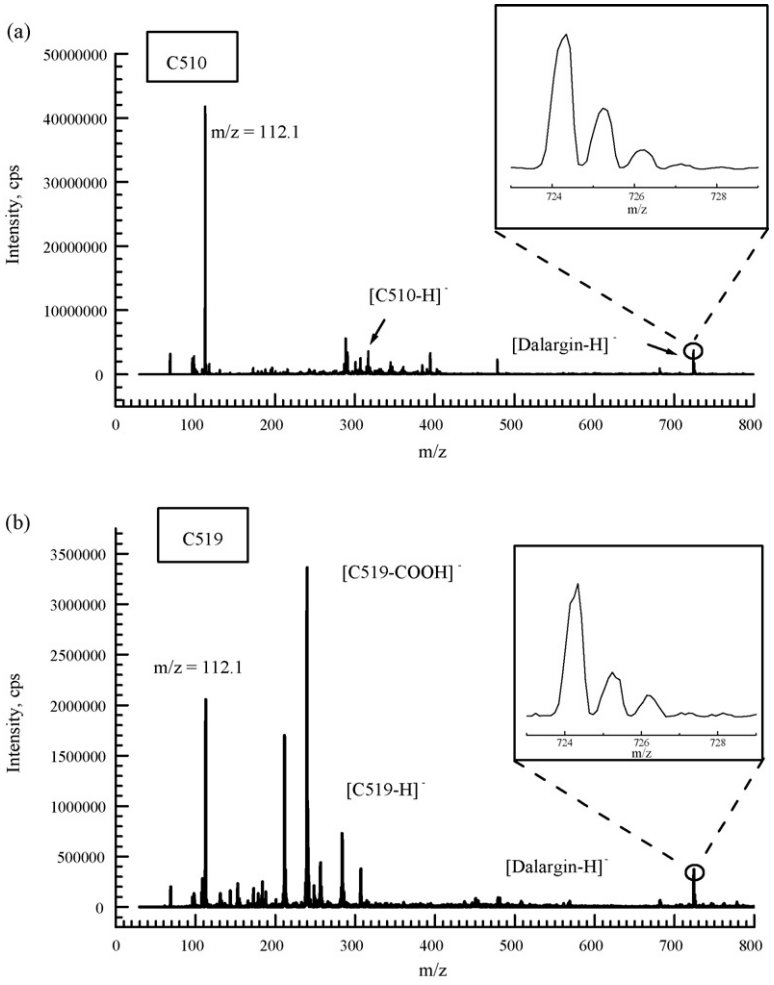

Fig. 4. Negative ion mode visible-MALDI mass spectrum of Dalargin in (a) C510 and (b) C519 using 480 nm light with energy = 60 μJ per pulse.

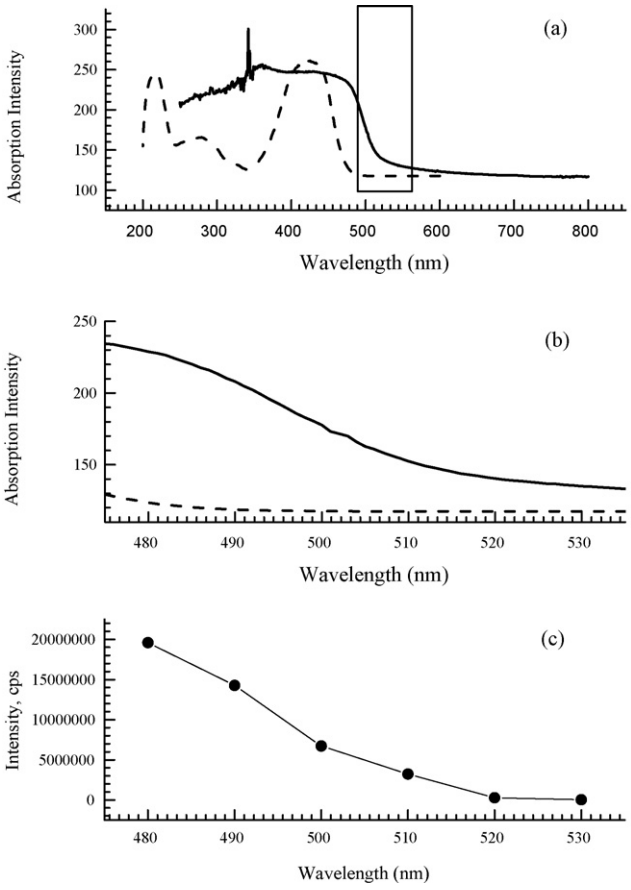

Fig. 5. Comparison of the diffuse reflectance spectrum for C510 for the solution (dashed line) and solid (solid line) phases. (a) Full UV–visible and diffuse reflectance spectrum for C510, (b) expanded view of the UV–visible and diffuse reflectance spectra in the long wavelength region, (c) intensity of protonated Dalargin ion signal seen in visible-MALDI spectra as a function of incident wavelength.

3.3. The effect of laser wavelength

Both UV and visible light was used to investigate the influence of laser wavelength on the efficacy of the C510 matrix. It is known that the molecular solid phase absorption spectrum can be considerably broadened and red-shifted [18] relative to that seen in liquid solutions, and can also display structure not seen in the solution spectra [19]. Both the solution C510 UV–visible spectrum and the diffuse reflectance spectrum of C510 are shown in Fig. 5(a). Similar to what has been previously observed for other UV–MALDI matrixes [20], the C510 absorption spectrum in the solid phase is indeed broadened relative to that observed in solution phase, covering the spectral range between 350 nm and 480 nm.

A range of laser wavelengths between 480 nm and 530 nm was selected to investigate the correlation between the intensity of the Dalargin MALDI signal and the absorption spectrum of the dye matrix. Fig. 5(b) and (c) shows clearly that the variation in the Dalargin MALDI ion intensity mirrors the absorption profile of the diffuse reflectance spectrum more closely than that of the solution UV–visible spectrum. As well, Dalargin MALDI signal were not readily detected for wavelengths outside the absorption profile of the solid dye. This correlation agrees more with similar studies done using UV versus IR wavelengths [21].

As shown in Fig. 6, and based on fluences studies described below similar Dalargin MALDI signals were expected in C510 using both 355 nm (UV; 20 μJ/pulse) and 480 nm (visible, 60 μJ/pulse) wavelengths. It appears however that the matrix is more strongly

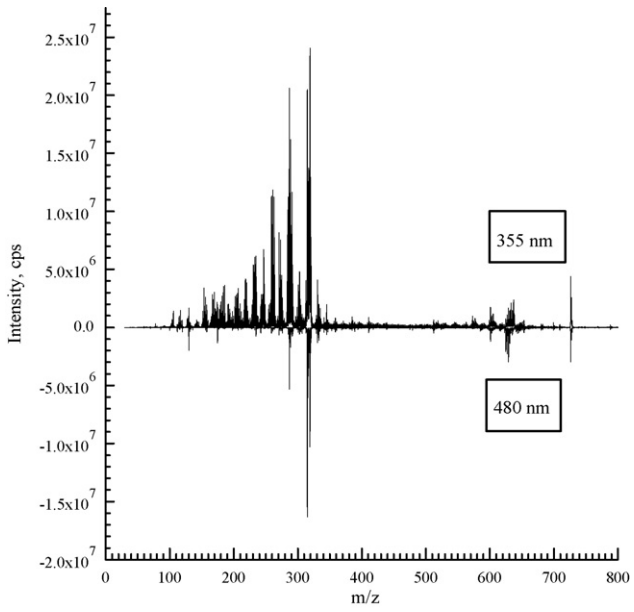

Fig. 6. UV and visible-MALDI spectrum of Dalargin in a C510 matrix taken with 355 nm (20 μJ per pulse) and 480 nm light (60 μJ per pulse), respectively. For comparison, the visible-MALDI spectrum is displayed with its intensity scale negative to that shown for the UV–MALDI spectrum.

fragmented under 355 nm radiation compared to that recorded using 480 nm light, and the analyte signal is weaker.

3.4. The effect of laser fluence

No significant changes were observed with respect to matrix fragmentation and cluster patterns for both dyes when the laser fluence was increased from 0.16 kJ/m^2 to 4 kJ/m^2. In these studies the laser spot size was fixed, and average matrix or analyte signals were collected. The absolute Dalargin and matrix-related ion signal intensities did increase with increasing laser fluence.

The log–log plots in Fig. 7 assume that the dependence of the MALDI signal intensity, S, on fluence, F, has the form $S \sim F^n$. In the case of non-resonant multiphoton ionization (MPI), the slopes of

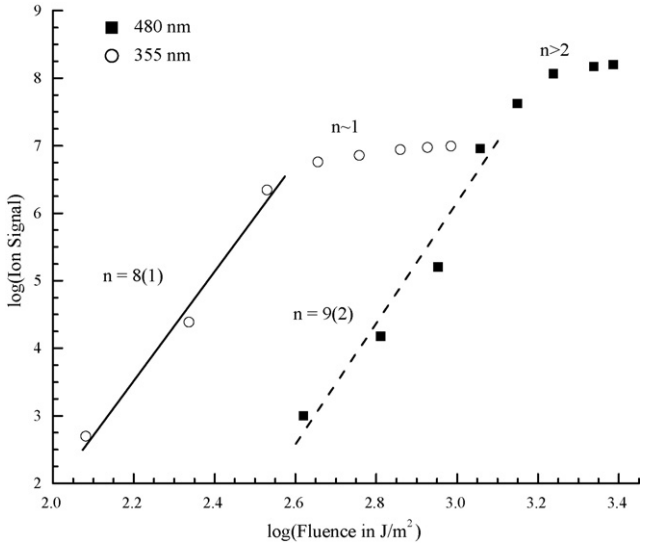

Fig. 7. A log–log plot of Dalargin MALDI signal intensity versus laser fluence at 355 nm and 480 nm.

such log–log plots, n, indicate the number of photons involved in the nonlinear absorption process [22]. The physical meaning of the slope in MALDI however is obscured by the fact that secondary reactions likely play a key role in determining the magnitude of the analyte signals. Each plot in Fig. 7 exhibits a behavior depending on the fluence level which is similar to the work of Westmacott et al. [23]. At low fluences the plots have large slopes ($n \sim 8$–9) while at higher fluences the slopes are smaller ($n \sim 1$ using 355 nm light and $n \geq 2$ at 480 nm). In either case it is unlikely that values of the former slopes correspond to the number of photons absorbed in the primary ionization step since the laser intensities used were not particularly high, and the total energy corresponding to even two or more photons if deposited into the matrix in the absorption step would leave a matrix molecule near or above its ionization potential.

4. Discussion and conclusions

Both C510 and C519 have been shown in this work to be suitable MALDI matrixes for the detection of selected peptides in both negative and positive ion modes using visible wavelength MALDI. The detection limits are comparable to those reported for conventional UV–MALDI using standard matrixes. The mode of anion ionization for C510 appears to be the abstraction of an acidic proton from Dalargin by the dye molecules or their fragments, resulting in the formation of $[M\text{-}H]^-$. The mode of positive ion formation using C510 is less clear but most likely it occurs via proton donation from a fragment of the matrix to the analyte.

The large slopes of log–log plots recorded at low fluences have been observed for other matrixes [23–25] irradiated by UV and IR sources. Conventional wisdom suggests that at low fluence ions are generated by molecular desorption while at higher fluences ablation will yield a mixture of clusters and molecules. Supporting evidence for this is the sensitivity of the fluence-signal intensity plot slopes to the focal spot size at the surface of the matrix. Ultimately saturation and a decline in ion signal is attributed to side reactions that lead to fragmentation, and detector saturation. The spot size used in this work leads to visible energy densities in near surface volumes that are on the order of typical combined heats of fusion and vaporization of matrix compounds. Thus, it can be concluded that the initial step leading to primary ion formation for the IR, visible and UV is similar, and most likely thermal in nature.

An additional observation from Fig. 7 is that a higher fluence is required for visible-MALDI operating in the lower ion yield regime compared to that required for UV illumination. The reason that the UV curve starts at lower fluences is attributed to the higher absorption coefficient at 355 nm which is clearly noticeable in Fig. 5. A higher absorption coefficient means a smaller penetration depth into the matrix and as a result, proportionally less energy is required to heat up desorbing material to the same temperature. A smaller absorption depth also means that less material is consumed per laser pulse and as a result fewer ions are created per pulse in the plateau region. This benefit for UV–MALDI is offset however by the softer ionization patterns associated with visible-MALDI, and consequently, the reduction in the mass interference in the low m/z region of the spectra.

Like C510, C519 has also been shown to be a suitable MALDI matrix for the detection of selected peptides in both negative and positive ion modes using visible wavelength MALDI, although anion analyte signals are stronger. In negative ion mode the C519 dye molecule appears to abstract an acidic proton from Dalargin, resulting in the formation of the $[C519\text{-}H]^-$ species. Cationization likely occurs via the donation of a proton from the carboxylic acid group on the dye molecule.

Ultimately, although MALDI using visible sources appears to yield reasonable results, it remains to be seen if higher mass analytes can be lifted and if the ultimate detection sensitivities approach those obtained by UV methods. A recent paper Chen et al. suggests that hundreds of femtomoles of heavier analytes can be detected using visible-MALDI-TOF [26]. Practically, the best visible dyes would be those that absorb 532 nm light (a doubled Nd:YAG laser output). Our group has examined several candidates which will be described in a later publication.

Acknowledgements

This work was supported by the Natural Sciences and Engineering Research Council of Canada (NSERC). The authors from Western are grateful to MDS-Analytical Technologies for their generous in-kind donation of the MALDI mass spectrometer to their lab.

References

[1] S. Berkenkamp, C. Menzel, M. Karas, F. Hillenkamp, Rapid Commun. Mass Spectrom. 11 (1997) 1399.
[2] R. Cramer, J.W. Richter, E. Stimson, A.L. Burlingame, Anal. Chem. 70 (1998) 4939.
[3] S. Niu, W. Zhang, B.T. Chait, J. Am. Soc. Mass Spectrom. 9 (1998) 1.
[4] D.R. Ermer, M. Baltz-Knorr, R.F. Haglund, J. Mass Spectrom. 36 (2001) 538.
[5] M.R. Papantonakis, J. Kim, W.P. Hess, R.F. Haglund Jr., J. Mass Spectrom. 37 (2002) 639.
[6] L.J. Romano, R.J. Levis, J. Am. Chem. Soc. 113 (1991) 9665.
[7] K. Tang, S.L. Allman, R.B. Jones, C.H. Chen, Org. Mass Spectrom. 27 (1992) 1389.
[8] C.J. Smith, S.Y. Chang, E.S. Yeung, J. Mass Spectrom. 30 (1995) 1765.
[9] D.S. Cornett, M.A. Duncan, I.J. Amster, Anal. Chem. 65 (1993) 2608.
[10] J. Kim, K. Paek, W. Kang, Bull. Korean Chem. Soc. 23 (2002) 315.
[11] Y.F. Huang, H.T. Chang, Anal. Chem. 78 (2006) 1485.
[12] I.K. Perera, S. Kantartzoglou, P.E. Dyer, Int. J. Mass Spectrom. Ion Processes 137 (1994) 151.
[13] I.K. Perera, S. Kantartzoglou, P.E. Dyer, Int. J. Mass Spectrom. Ion Processes 156 (1996) 151.
[14] D. Lacey, X.K. Hu, A.V. Loboda, N.J. Mosey, R.H. Lipson, Int. J. Mass Spectrom. 261 (2007) 192.
[15] T.-D.W. Chan, A.W. Colburn, P.J. Derrick, Org. Mass Spectrom. 26 (1991) 342.
[16] T.-D.W. Chan, A.W. Colburn, P.J. Derrick, J.D. Gardiner, M.M. Bowden, Org. Mass Spectrom. 27 (1992) 188.
[17] D. Lacey, Experiments in VUV and visible wavelength MALDI using a triple quadrupole mass spectrometer, Ph.D. thesis, The University of Western Ontario, 2006.
[18] V. Horneffer, K. Dreisewerd, H.-C. Lüdemann, F. Hillenkamp, M. Läge, K. Strupat, Int. J. Mass Spectrom. 185–187 (1999) 859.
[19] D.A. Allwood, R.W. Dreyfus, I.K. Perera, P.E. Dyer, Rapid Commun. Mass Spectrom. 10 (1996) 1575.
[20] K. Strupat, M. Karas, F. Hillenkamp, Int. J. Mass Spectrom. Ion Processes 111 (1991) 89.
[21] J.D. Sheffer, K.K. Murray, Rapid Commun. Mass Spectrom. 12 (1998) 1685.
[22] S.L. Chin, Phys. Rev. A 4 (1971) 992.
[23] G. Westmacott, W. Ens, F. Hillenkamp, K. Dreisewerd, M. Schurenberg, Int. J. Mass Spectrom. 221 (2002) 67.
[24] W. Ens, Y. Mao, F. Mayer, K.G. Standing, Rapid Commun. Mass Spectrom. 5 (1991) 117.
[25] K. Dreisewerd, M. Schürenberg, M. Karas, F. Hillenkamp, Int. J. Mass Spectrom. Ion Processes 141 (1995) 127.
[26] L.C. Chen, D. Asakawa, H. Hori, K. Hiraoka, Rapid Commun. Mass Spectrom. 21 (2007) 4129.